Impact-induced glass-to-rubber transition of polyurea under high-velocity temperature-controlled microparticle impact

Impact-induced glass-to-rubber transition of polyurea under high-velocity temperature-controlled microparticle impact

Yuchen Sun,[1,2] Steven E. Kooi,[1] Keith A. Nelson,[1,2] Alex J. Hsieh,[1,3] and David Veysset[1,a)]

AFFILIATIONS

[1]Institute for Soldier Nanotechnologies, Massachusetts Institute of Technology, Cambridge, Massachusetts 02139, USA

[2]Department of Chemistry, Massachusetts Institute of Technology, Cambridge, Massachusetts 02139, USA

[3]U.S. Army Combat Capabilities Development Command, Army Research Laboratory, FCDD-RLW-MG, Aberdeen Proving Ground, MD 21005-5069, USA

[a)]Author to whom correspondence should be addressed: dveysset@mit.edu

ABSTRACT

Deformation-induced glass transition in segmented elastomers has been proposed to allow highly-desirable enhanced energy dissipation. In this study, we investigate the temperature-dependent micro-scale impact response of polyurea at a fixed impact velocity. We observe a local elevated impact energy absorption around 115°C, which is attributed to the glass-to-rubber transition temperature under the present high-rate dynamic loading. Dielectric spectroscopy was performed and the soft-segmental α_2-relaxation was extracted and fit with a Havriliak–Negami function. The α_2-relaxation frequency at 115°C correlates well with an order-of-magnitude estimate of the equivalent frequency of deformation. This work further supports the importance of the dynamical T_g as an important consideration in the design of impact resistant materials.

High mechanical energy absorption in lightweight materials is a greatly desirable trait for many commercial applications involving high strain rate deformations such as helmets, automotive crashworthiness materials, and impact-resistant devices[1–3]. Elastomers offer desirable properties in such applications including high mechanical damping capabilities, remarkable toughness, high chemical resistance, and low cost[3,4]. Polyurea, in particular, was shown to exhibit a uniquely robust ballistic impact response, purportedly as a result of its propensity to undergo a strain-rate-induced glass transition under ballistic impact[5,6]. This discovery led to a heightened interest in the high-strain-rate responses of various segmented elastomers including polyurea, polyurethane, and poly(urethane urea)[5,7–13]. Through control of molecular moieties, one can design these hierarchical elastomers to express different degrees of separation and mixing (incomplete segment segregation) between the hard and soft segment phases, which directly impact the segmental relaxation dynamics and therefore the rate-dependent mechanical behavior[9,14,15].

In polyurea synthesized with a poly(tertramethylene oxide) (PTMO) soft segment molecular weight of 650 g/mol (thereafter named PU650), segmental motions attributed to soft segments were shown to consist of two α-relaxations: a fast segmental motion (α_1) related to unrestricted motion of soft segments in the soft-segment rich phase and a slower motion related to constrained soft segments attached to hard domains (α_2)[16]. For a quasi-static deformation rate (10^{-2} s^{-1}), Castagna et al. estimated the glass transition temperatures T_g associated with the α_1-relaxation and the α_2-relaxation processes to be -53°C and 22°C, respectively[16]. For higher deformation rates, the glass transition temperatures shift toward higher values following a Vogel-Fulcher-Tammann law; the higher-rate transitions are often referred to as "dynamic glass transitions". It is well known that energy dissipation is significantly increased at the glass transition temperature[17]. Based on this premise, Bogoslolov & Roland demonstrated that a strain-rate-induced glass transition leads to enhanced energy dissipation upon impact of elastomers for which the characteristic deformation rate is comparable to the segmental relaxation kinetics, which in their study corresponded to the α_1-relaxation[5].

Most studies focusing on the high-rate response of hierarchical polymers rely on broadband dielectric spectroscopy as a well-established tool that can reach frequencies up to 10^7 s^{-1}, thereby guiding the design of impact-resistant materials[18–20]. However, few experimental works have directly validated this guidance through direct measurements of high-velocity impact. The development and use of the laser-induced particle impact test

(LIPIT), a microballistic platform[21], has yielded extensive impact data on segmented elastomers[10,13] reaching strain-rates of ~10^8 s^{-1}. These micro-impact studies have demonstrated the importance of intersegmental mixing and hydrogen bonding networks in the high-strain-rate responses of the elastomers[11,12,22]. In this study, we investigate the high-strain-rate glass transition of polyurea by conducting temperature-controlled experiments at a fixed micro-impact velocity. We aim to directly measure the dynamic glass-to-rubber transition associated with the relaxation dynamics of constrained soft segments near the hard phase, which were reported to correspond to the α_2-relaxation in polyurea[16]. Our results represent the first LIPIT high-velocity microscale impacts at non-ambient temperatures and direct measurements of a dynamic phase transition temperature at the associated high strain rates.

The polyurea target was synthesized in a 1:1 stoichiometric ratio of a modified curative, polycarbodiimide-modified diphenylmethane diisocyanate (MDI) (Isonate 143L, RCS Rocket Motor Components) and an oligomeric diamine (Versalink® P650), based on poly(tetramethylene oxide di-p-aminobenzoate) (PTMO) with a molecular weight of 650 g/mol (obtained from Evonik). After mixing, the reactants were cast between two glass plates with a 1-mm thick rubber spacer and polymerized at room temperature for 48 days. The specimen was then placed in a desiccator for 8 days and aged for more than 14 days prior to testing[16,23]. Sample heating was achieved with a resistive heating plate with a polyimide conduction surface (Icstation, 12V, 7W), controlled by a digital proportional-integral-derivative (PID) thermostat (Inkbird, ITC-100VL). The polyurea sample was secured to the heating plate with adhesive tape along the edges. Temperature was measured with a thermocouple at the top surface of the target and used as feedback into the PID thermostat.

Microparticle impact experiments were conducted using the LIPIT platform, schematically represented in Fig. 1. First, a launch pad is assembled by depositing a gold film (60-nm thick) and spin-coating a polymer film (polyurea, 30-μm thick) onto a glass substrate (210 μm thick). This assembly is kept under vacuum for 24 hours and then cured at 85°C for 18 hours. Silica spheres (7.4-μm diameter) are deposited and dispersed across the surface of the polymer film. Prior to each launch, a single silica sphere is selected for acceleration using a CCD camera. Acceleration is achieved via ablation of the sacrificial gold film with a high-energy laser pulse (Nd-YAG, 532-nm wavelength, 10-ns duration). Ablation induces a rapid expansion of the polymer film which

subsequently accelerates the particle into free space toward the target, placed around 2 mm away from the launching pad. The trajectory of the particle, both prior to and after impact, is observed with a microscope (10× objective, 40-cm tube lens) and an ultra-high-speed multi-frame camera (SIMX16, Specialized Imaging). The illumination is provided by a second laser pulse (640-nm wavelength, 30-µs duration). The camera yields a 16-frame sequence of the impact event with variable interframe time and a minimum exposure time of 5 ns. More details regarding the launch pad preparation and the optical system can be found in our previous works[13,24].

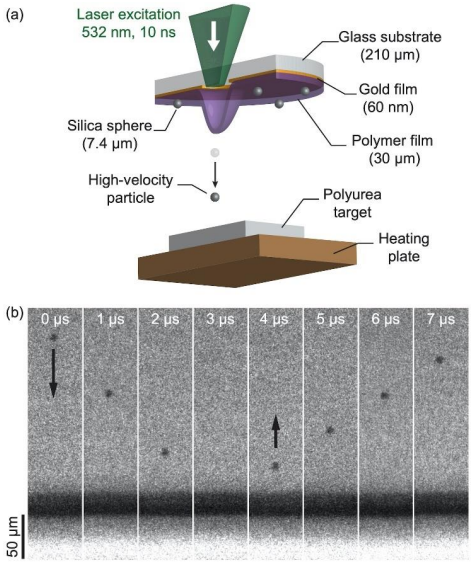

FIG. 1. (a) Schematic representation of the LIPIT platform. A particle is accelerated toward a polyurea target following ablation of a sacrificial gold film with a high-energy laser pulse. (b) Representative image sequence of a silica sphere (7.4 µm) impacting a polyurea target at 23°C. The impact and rebound velocities are measured to be 65 m/s and 39 m/s, respectively.

A representative image sequence of a silica sphere impacting the polyurea target at 23°C is shown in Fig. 1b. From this image sequence, the impact and subsequent rebound velocities were measured to be 65 m/s and 39 m/s, respectively. The coefficient of restitution, the ratio between rebound V_r and impact velocities V_i, was calculated to be 0.60. In this study, a series of impacts was performed within a tight range of impact velocities

(60-72 m/s) while varying the target temperature from 23°C (room temperature) to nearly 160°C. To better resolve temperature effects on the coefficient of restitution, we chose a velocity range for which the coefficient of restitution value is high at room temperature[12]. Within this impact velocity range, the coefficient of restitution varies by less than 3% as a function of impact velocity at constant temperature. The coefficient of restitution variation with temperature is shown in Fig. 2a. Variation of the coefficient of restitution as a function of temperature has been used to study the dynamic glass-to-rubber transition in polymers, where a pronounced change in energy absorption upon impact is observed at the transition temperature[25–28].

A minimum in the coefficient at ~115°C corresponds to a maximum in relative energy absorption $\%E_a$, calculated as $\%E_a=1-V_r^2/V_i^2$ (Fig. 2b). As temperature increases, the polyurea target behavior transitions from glassy-like to leathery, corresponding to the maximum observed energy absorption, and eventually to rubbery-like with a slightly lower energy absorption. We define a first-order characteristic contact time t_c as the sum of the time to reach full penetration h_{max} and the time to detach from the sample, assuming a penetration velocity of V_i and an exit velocity of V_r:

$$t_c = h_{max}\left(\frac{1}{V_i}+\frac{1}{V_r}\right) \quad (1)$$

Because of the shadow cast by the sample, it is not possible to image the penetration of the particle inside the target close to the surface and thus h_{max} is not measured in our experiments. We can however anticipate the penetration depth to be on the order of a few microns or less based on previous experiments performed on similar materials[10].

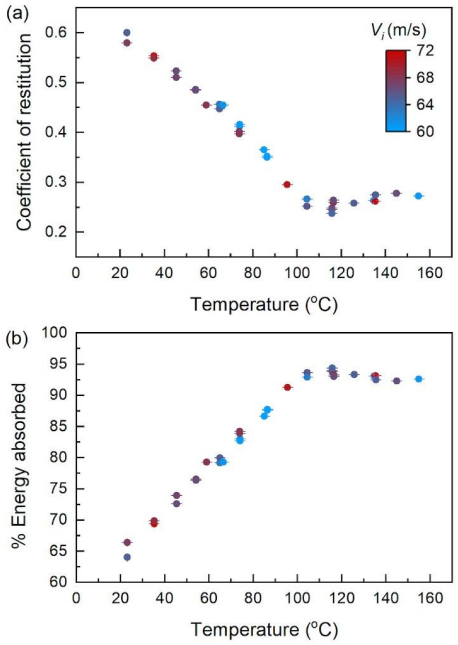

FIG. 2. (a) Coefficient of restitution (COR) as a function of target temperature for impacts around 65 m/s onto the polyurea target. The COR decreases rather smoothly with increasing temperature until it reaches a minimum at around 115°C and then increases slightly at higher temperatures. The minimum is indicative of a dynamic glass-to-rubber transition. (b) Percentage energy absorbed during impact a function of temperature.

Dielectric relaxation measurements were carried out using a Novocontrol Concept 40 Broadband Dielectric Spectrometer to characterize the material segmental dynamics and identify the relevant relaxation times. A polyurea specimen (0.54-mm thick), sputter-coated with a thin gold layer (5-nm thick) on both sides, was sandwiched between two 1-cm diameter brass electrodes to form a parallel-plate capacitor. Measurements were conducted isothermally with an AC voltage V_{rms} of 1.5 V with specimen temperatures varying from -20°C to 130°C (5°C steps) and applied frequencies from 10^{-1} to 10^{6} Hz. We follow the procedure described by Fragiadakis and Runt to analyze the dielectric results[19]. The derivative representation ε_D of the dielectric permittivity is shown in Fig. 3 with:

$$\varepsilon_D = -\frac{\pi}{2}\frac{d\,\varepsilon'}{d\ln\omega} \qquad (2)$$

The derivative form of the permittivity allows a better visualization of the relaxation processes by eliminating dc conduction losses, which obscure the loss peaks in the measured ε'' data. From the dielectric spectrum, presented in Fig. 3, we identify the peak characteristic of the α_2-relaxation corresponding to the constrained soft segmental motions. We note that the α_1-relaxation is not pronounced over the studied temperature and frequency range as also suggested by Castagna et al.[16]

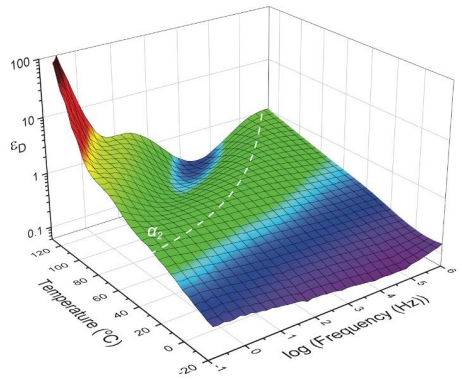

FIG. 3. Derivative representation of the dielectric relaxation data ε_D as a function of temperature and frequency revealing the locus of the α_2-relaxation peak.

The frequency of the maximum α-relaxation mode, f_{max}, can be extracted by fitting the dielectric loss ε'' with a Havriliak–Negami function[29]:

$$\varepsilon^* = \varepsilon' - i\varepsilon'' = \varepsilon_\infty + \frac{\Delta\varepsilon}{(1+(if/f_{HN})^m)^n} \qquad (3)$$

where ε_∞ is the infinite-frequency dielectric constant, $\Delta\varepsilon$ is the dielectric strength, m and n are shape parameters related to the breadth of the relaxation and the high frequency asymmetry, respectively, and f_{HN} is a characteristic frequency. The dielectric strength, the width and shape parameters, and the characteristic frequency were fitted for all temperatures. The fit at 115°C is shown in Fig. 4, along with the dielectric data at that temperature.

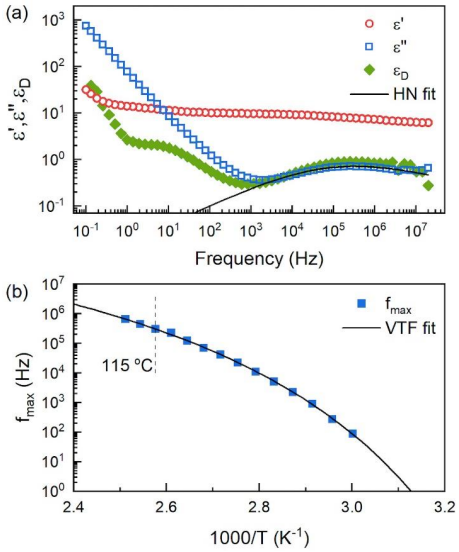

FIG. 4. (a) Dielectric spectra for polyurea at 115°C. Real and imaginary parts (open symbols) and derivative ε_D. The α_2-relaxation peak is fitted with a Havriliak–Negami (HN) function (b) Arrhenius plot of segmental relaxation peak frequency (f_{max}) data fitted with Vogel-Fulcher-Tammann function.

The characteristic frequency f_{HN} is related to the frequency of the maximum loss f_{max} through:

$$f_{max} = f_{HN}\left(\frac{\sin\frac{\pi m}{2+2n}}{\sin\frac{\pi mn}{2+2n}}\right)^{1/m} \quad (4)$$

The obtained f_{max} values shown in Fig. 4 give the temperature-dependence of the maximum loss frequency. The α-relaxation obeys a Vogel-Fulcher-Tammann (VFT) temperature dependence with:

$$f_{max} = f_0 \exp\left(\frac{-B}{T-T_0}\right) \quad (5)$$

where f_0, B and T_0 (Vogel temperature) are constants. The fit yielded $f_0 = 10^{10}$ Hz, $B = 1300$ K^{-1}, and $T_0 = 263$ K. The α_2-relaxation peak frequency measured at around 115°C (± 5°C) is in the range 2–5×10^5 Hz. The corresponding relaxation time, τ, is calculated to be ~500 ns, from the relation $\tau = 1/2\pi f_{max}$.[30]

Assuming, as a first order, that the impact is a half cycle of a sinusoidal vibration, we can calculate the equivalent frequency of the experiment to be $f_{impact} = ½\, t_c$. In the absence of direct measurement for penetration

depth, we assume h_{max} to be the particle diameter and estimate f_{impact}~8×10^5 Hz (Eq. 1). The concept of equivalent frequency has been proposed decades ago[25] and is simplistic in nature as it eludes the range of frequencies achieved during impact. However, it provides a reasonable order-of-magnitude approximation[25] and allows us to compare it with the α_2-relaxation frequency f_{max} and thus to validate that we are probing the α_2 dynamics of the soft segments near the interface. Furthermore, based on the dielectric measurements performed by Castagna et al., we anticipate that, for impacts at 65 m/s, we would observe the glass transition corresponding to the α_1-relaxation at about -5°C. Future efforts will be dedicated into implementing a cooling stage to support this hypothesis.

In summary, through microparticle impact measurements on a temperature-controlled polyurea target, we directly measure the dynamic glass-to-rubber transition temperature of polyurea at a high strain rate (~10^5 s^{-1}). Dielectric spectroscopy results confirm that the observed transition corresponds to the α_2-relaxation of the soft segments near the hard-segment interfaces. Our results align with those of Bogoslovov & Roland [5], which showed that molecular relaxation is induced when the segmental dynamics become comparable to the mechanical strain rate, resulting in increased energy dissipation. This work further supports the importance of the dynamic T_g in impact mitigation and indicates that the results should help guide the design of impact-resistant materials.

The data that support the findings of this study are available from the corresponding author upon reasonable request.

YS and DV thank Juliana Cherston (MIT) for lending the plate heater and temperature controller. This material is based upon work supported by the U.S. Army Combat Capabilities Development Command, Army Research Office and Army Research Laboratory through the Institute for Soldier Nanotechnologies, under Cooperative Agreement No. W911NF-18-2-0048.

REFERENCES

[1] F.M. Shuaeib, A.M.S. Hamouda, M.M. Hamdan, R.S. Radin Umar, and M.S.J. Hashmi, J. Mater. Process. Technol. **123**, 432 (2002).

[2] S.G. Kulkarni, X.-L. Gao, S.E. Horner, J.Q. Zheng, and N.V. David, Compos. Struct. **101**, 313 (2013).

[3] M.-Y. Lyu and T.G. Choi, Int. J. Precis. Eng. Manuf. **16**, 213 (2015).

[4] S. Song, J. Feng, P. Wu, and Y. Yang, Macromolecules **42**, 7067 (2009).

[5] R.B. Bogoslovov, C.M. Roland, and R.M. Gamache, Appl. Phys. Lett. **90**, 221910 (2007).

[6] M. Grujicic, B. Pandurangan, T. He, B.A.A. Cheeseman, C.-F.F. Yen, and C.L.L. Randow, Mater. Sci. Eng. A **527**, 7741 (2010).

[7] D. Fragiadakis, R. Gamache, R.B.B. Bogoslovov, and C.M.M. Roland, Polymer **51**, 178 (2010).

[8] A.J. Hsieh, T.L. Chantawansri, W. Hu, K.E. Strawhecker, D.T. Casem, J.K. Eliason, K. a. Nelson, and E.M. Parsons, Polymer **55**, 1883 (2014).

[9] R.G. Rinaldi, A.J. Hsieh, and M.C. Boyce, J. Polym. Sci. Part B Polym. Phys. **49**, 123 (2011).

[10] D. Veysset, A.J. Hsieh, S.E. Kooi, and K.A. Nelson, Polymer **123**, 30 (2017).

[11] Y.-C.M. Wu, W. Hu, Y. Sun, D. Veysset, S.E. Kooi, K.A. Nelson, T.M. Swager, and A.J. Hsieh, Polymer **168**, 218 (2019).

[12] Y. Sun, Y.-C.M. Wu, D. Veysset, S.E. Kooi, W. Hu, T.M. Swager, K.A. Nelson, and A.J. Hsieh, Appl. Phys. Lett. **115**, 093701 (2019).

[13] D. Veysset, A.J. Hsieh, S. Kooi, A.A. Maznev, K.A. Masser, and K.A. Nelson, Sci. Rep. **6**, 25577 (2016).

[14] W. Hu and A.J. Hsieh, Polymer **54**, 6218 (2013).

[15] W. Hu, N. V. Patil, and A.J. Hsieh, Polymer **100**, 149 (2016).

[16] A.M. Castagna, A. Pangon, T. Choi, G.P. Dillon, and J. Runt, Macromolecules **45**, 8438 (2012).

[17] E. Riande, D.-C. Ricardo, M. Prolongo, R. Masegosa, and C. Salom, *Polymer Viscoelasticity* (CRC Press, 1999).

[18] A.M. Castagna, D. Fragiadakis, H. Lee, T. Choi, and J. Runt, Macromolecules **44**, 7831 (2011).

[19] D. Fragiadakis and J. Runt, Macromolecules **46**, 4184 (2013).

[20] A.J. Hsieh, T.L. Chantawansri, W. Hu, J. Cain, and J.H. Yu, Polymer **95**, 52 (2016).

[21] J.-H. Lee, D. Veysset, J.P. Singer, M. Retsch, G. Saini, T. Pezeril, K.A. Nelson, and E.L. Thomas, Nat. Commun. **3**, 1164 (2012).

[22] A.J. Hsieh, D. Veysset, D.F. Miranda, S.E. Kooi, J. Runt, and K.A. Nelson, Polymer **146**, 222 (2018).

[23] K. Holzworth, Z. Jia, A. V. Amirkhizi, J. Qiao, and S. Nemat-Nasser, Polymer **54**, 3079 (2013).

[24] M. Hassani-Gangaraj, D. Veysset, K.A. Nelson, and C.A. Schuh, Scr. Mater. **145**, 9 (2018).

[25] H.H. Calvit, J. Mech. Phys. Solids **15**, 141 (1967).

[26] J. Pouyet and J.L. Lataillade, J. Mater. Sci. **10**, 2112 (1975).

[27] G. Constantinides, C.A. Tweedie, D.D.M. Holbrook, P. Barragan, J.F.J. Smith, and K.K.J. Van Vliet, Mater. Sci. Eng. A **489**, 403 (2008).

[28] J. Diani, P. Gilormini, and G. Agbobada, J. Mater. Sci. **49**, 2154 (2014).

[29] S. Havriliak and S. Negami, J. Polym. Sci. Part C Polym. Symp. **14**, 99 (1966).

[30] F. Kremer, A. Schönhals, and A. Schonhals, *Broadband Dielectric Spectroscopy* (Springer Berlin Heidelberg, Berlin, Heidelberg, 2003).

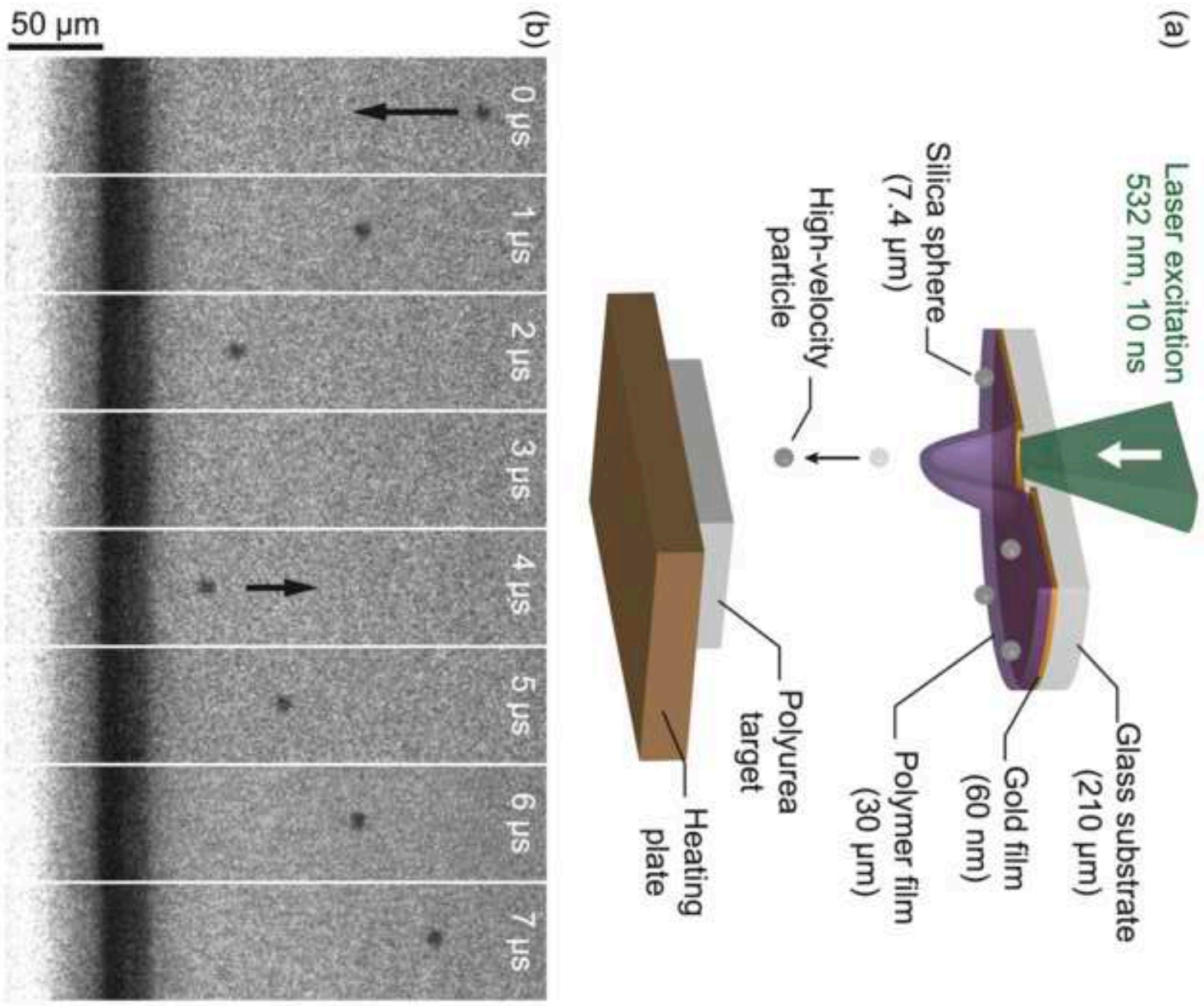

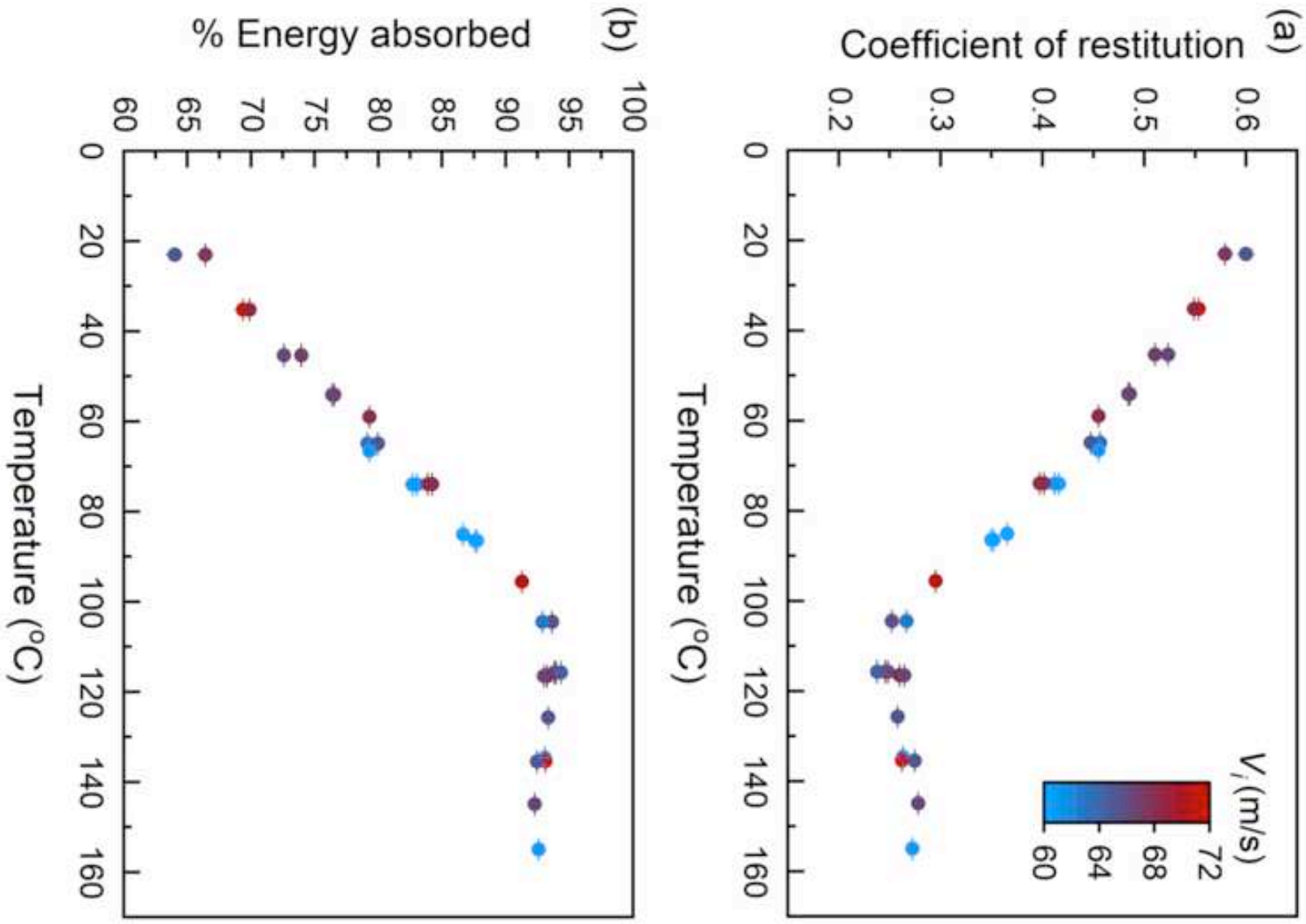

PLEASE CITE THIS ARTICLE AS DOI: 10.1063/5.0013081